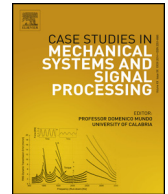




ELSEVIER

Contents lists available at ScienceDirect

# Case Studies in Mechanical Systems and Signal Processing

journal homepage: [www.elsevier.com/locate/csmssp](http://www.elsevier.com/locate/csmssp)

Short communication

## A comparative study of adaptive filters in detecting a naturally degraded bearing within a gearbox

Faris Elasha<sup>a,\*</sup>, David Mba<sup>b</sup>, Cristobal Ruiz-Carcel<sup>c</sup><sup>a</sup> School of Mechanical, Automotive and Aerospace Engineering, Coventry University, UK<sup>b</sup> School of Engineering, London South Bank University, UK<sup>c</sup> School of Aerospace, Transport and Manufacturing, Cranfield University, UK

## ARTICLE INFO

## Article history:

Received 5 October 2015

Received in revised form 23 October 2015

Accepted 17 November 2015

Available online 28 November 2015

## Keywords:

Vibration analysis

Condition monitoring

Fault

Bearing

Adaptive filters

Signal processing

Gearbox

Diagnostics

## ABSTRACT

The diagnosis of bearing faults at the earliest stage is critical in avoiding future catastrophic failures. Many diagnostic techniques have been developed and applied in for such purposes, however, these traditional diagnostic techniques are not always successful when the bearing fault occurs within a gearbox where the vibration response is complex; under such circumstances it may be necessary to separate the bearing vibration signature.

This paper presents a comparative study of four different techniques for bearing signature separation within a gearbox. The effectiveness of these individual techniques were compared in diagnosing a bearing defect within a gearbox employed for endurance tests of an aircraft control system. The techniques investigated include the least mean square (LMS), self-adaptive noise cancellation (SANC) and the fast block LMS (FBLMS). All three techniques were applied to measured vibration signals taken throughout the endurance test. In conclusion it is shown that the LMS technique detected the bearing fault earliest.

© 2015 The Authors. Published by Elsevier Ltd. This is an open access article under the CC BY-NC-ND license (<http://creativecommons.org/licenses/by-nc-nd/4.0/>).

### 1. Introduction

Monitoring of machine vibration for early fault detection is widely applied [1,2]. The vibration signals from machines contain multiple sources which can be corrupted by noise from the transmission path. The diagnosis of bearing faults in gearboxes is not without its challenges [3,4], therefore methods of enhancing the signal to noise ratio (SNR) are required [5]. This is particularly the case in gearboxes where the gear mesh contribution to the overall vibration is of such significance as to mask bearing fault frequencies [6,7]. In practice, envelope analysis has been used to extract the bearing fault vibration signature in gearboxes, though in some cases envelope analysis has failed to reduce the gear mesh contribution to the total vibration signal. In such instances a narrow band-pass filter at high frequency has been applied to separate the high frequency component excited by bearing impacts [8].

Recently, signal separation techniques have been applied in the diagnosis of bearing faults within gearboxes. The separation is based on decomposing the signal into deterministic and random components. The deterministic part represents the gear component and the random part represents the bearings component of vibration. The bearing contribution to the signal is expected to be random due to slip effects [9].

\* Corresponding author.

E-mail addresses: [faris.elasha@coventry.ac.uk](mailto:faris.elasha@coventry.ac.uk), [farismoh2005@yahoo.com](mailto:farismoh2005@yahoo.com) (F. Elasha).

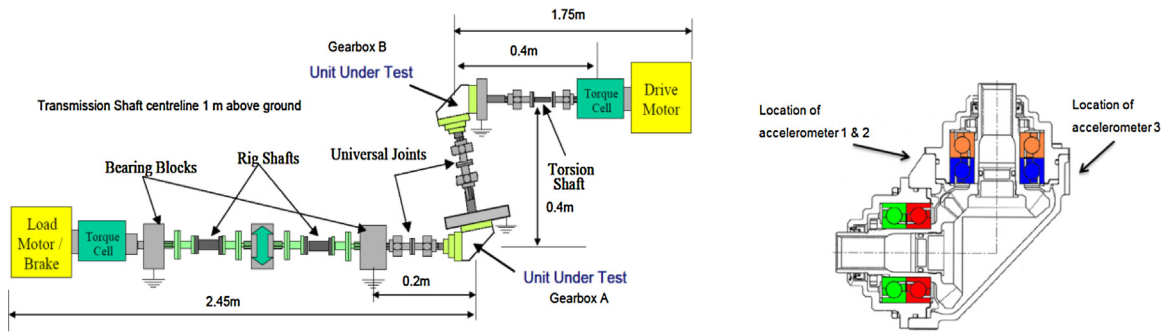


Fig. 1. Test rig layout (left) and gearbox configuration (right).

Table 1

Load cycles characteristics summary.

Cycle type	1	2	3	4	5	6	7	8	9
Times applied during bearing life	18296	22869	4574	462	462	2200	6600	4620	41580
Duration (s)	131	131	131	350	42	71	268	52	52
Torque max. (Nm)	126.1	126.1	158.6	126.1	126.1	42.8	42.8	12.4	97.7

More recently, the use of adaptive filters has been applied to monitor bearings [10,11]. This concept is based on the Wold Theorem, in which the signal can be decomposed into deterministic and non-deterministic parts [12]. The separation is based on the fact that the deterministic part has a longer correlation than the random part and therefore the autocorrelation is used to distinguish the deterministic part from the random part. However a reference signal is required to perform the separation. The application of this theory in condition monitoring was established by Chaturvedi et al. [13] where the Adaptive noise cancellation (ANC) algorithm was applied to separate bearing vibrations corrupted by engine noise with the bearing vibration signature used as a reference signal for the separation process. However, for practical diagnostics, the reference signal is not always readily available. As an alternative a delayed version of the signal has been proposed as a reference signal and this method is known as Self-adaptive noise cancellation (SANC) [14] which is based on delaying the signal until the noise correlation is diminished and only the deterministic part is correlated.

Three algorithms were compared to assess their effectiveness in diagnosing a bearing defect in a gearbox; least mean square (LMS), self-adaptive noise cancellation (SANC) and fast block LMS (FBLMS). These algorithms were applied to decompose the measured vibration signal into deterministic and random parts with the latter containing the bearing signal. This investigation assesses the merits of these techniques in identifying a natural degraded bearing under conditions of relatively large background noise. The gearbox considered in this study is part of a transmission system of an aircraft control system which suffered premature bearing failure at an early stage of testing; therefore, these algorithms will be applied to examine their ability to identify the failure at the onset of degradation.

## 2. Theoretical background

### 2.1. Adaptive filter

An adaptive filter is used to model the relationship between two signals in an iterative manner; the adaption refers to the method used to iterate the filter coefficient. The adaptive filter solution is not unique however the best solution is that which is closest to the desirable response signal. FIR filters are more commonly used as adaptive filters in comparison of IIR filters [15].

Table 2

Bearing faults frequencies.

Parts	Frequency (Hz)
Shaft speed frequency (SS)	11.8
Gear mesh frequency (GM)	201.2
Inner race defect frequency (IRD)	83.2
Outer race defect frequency (ORD)	58.8
Cage defect frequency	4.9
Ball spin frequency	25.6
Rolling element defect frequency	51.2

**Table 3**  
Maximum kurtosis location.

Observation	$F_c$ (Hz)	$\Delta f$ (Hz)	$K_{max}$	Frequency band (Hz)
1	2083.33	833.3	2.4	1666.7–2500
2	2083.33	833.3	2.4	1666.7–2500
3	2083.33	833.3	1.7	1666.7–2500

The adaptive filter concept is based on Wold theorem which proposes that the vibration signal can be decomposed into two parts, deterministic  $P(n)$  and random  $r(n)$ . This decomposition process can be represented by the following formula [12]:

$$x(n) = P(n) + r(n) \tag{1}$$

In the equation above the deterministic part can be predicted based on the history of the signal and the minimal prediction error, however the random part component cannot be predicted. The process of separation begins by applying adaptive noise cancellation (ANC), the fundamentals of this method have been detailed in [16].

2.2. Self-adaptive noise cancellation

SANC has been proposed to overcome the problem applying ANC algorithm for fault diagnosis of bearings. The problem with the ANC method, as applied to bearing fault detection in real applications, is that it is not always easy to identify the source of noise  $n_1$  which is correlated with the noise  $n_0$  (common source) but not with the fault signal. Chaturvedi et al. [13] presented an example where the method was applied to detect an induced bearing fault in a gearbox using two sensors; one was placed in the surroundings of the bearing housing to obtain the main signal and another sensor was placed at a remote location in the casing of the gearbox to obtain the reference signal. To solve this issue, a further development of ANC was formulated using a delayed version of the primary signal [14]. This latter version was named the SANC, full description of this method was detailed by Ho et al. [14].

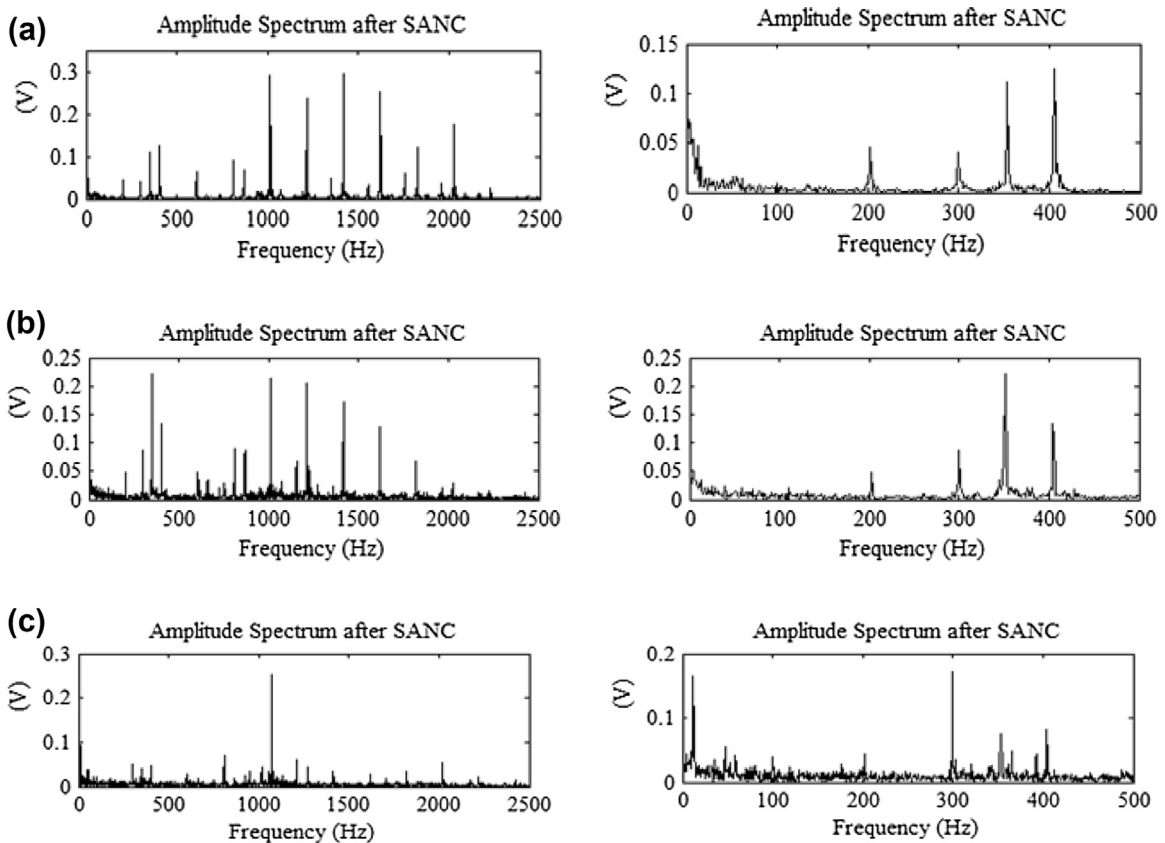


**Fig. 2.** (a) SANC first observation (24% of bearing life), (b) SANC second observation (27% of bearing life) and (c) SANC third observation (30% of bearing life).

### 2.3. LMS algorithm

The objective of the LMS algorithm is to optimize filter parameters and minimize prediction error, the prediction error  $\varepsilon_n$  is estimated according by [17]:

$$\varepsilon_n = d_n - h_i \times x(n - i) \quad (2)$$

where,  $d_n$  denotes the desirable signal. The filter coefficient should be adjusted to minimize this error function. These coefficient are updated by:

$$h_{n+1} = h_n + 2\mu x(t)\varepsilon \quad (3)$$

In which,  $h_{n+1}$  denote the updated filter coefficient, and  $\mu$  denotes the step size of the filter, this parameter should be selected carefully, the larger the step size the faster convergence, whilst on other hand a smaller step size leads to more accurate prediction, optimisation of step size was discussed in [16]. In addition, the filter length should be selected carefully, the largest size filter decreases convergence speed and *vice versa*.

### 2.4. Fast block LMS algorithm

Applying of the standard LMS algorithm to adaptive filtering results in long processing time, this due to coefficients been updated sample by sample. This delay limits the use of the LMS algorithm for real time applications, therefore the Fast block LMS (FBLMS) algorithm was proposed to reduce the process time [18]. This algorithm is based on the transforming the time signal to the frequency domain and the filter coefficient is updated after transformation. In this algorithm the filter coefficient is updated for each segment, whereas the LMS algorithm updates the coefficients for each sample. The detail procedure of FBLMS is summarised in [19].

### 2.5. Spectral kurtosis and envelope analysis

The basic principle of this method is to calculate the kurtosis at different frequency bands in order to identify non stationarities in the signal and determine where they are located in the frequency domain. Obviously the results obtained strongly depend on the width of the frequency bands  $\Delta f$  [20]. Antoni [20] suggested a methodology for the fast computation

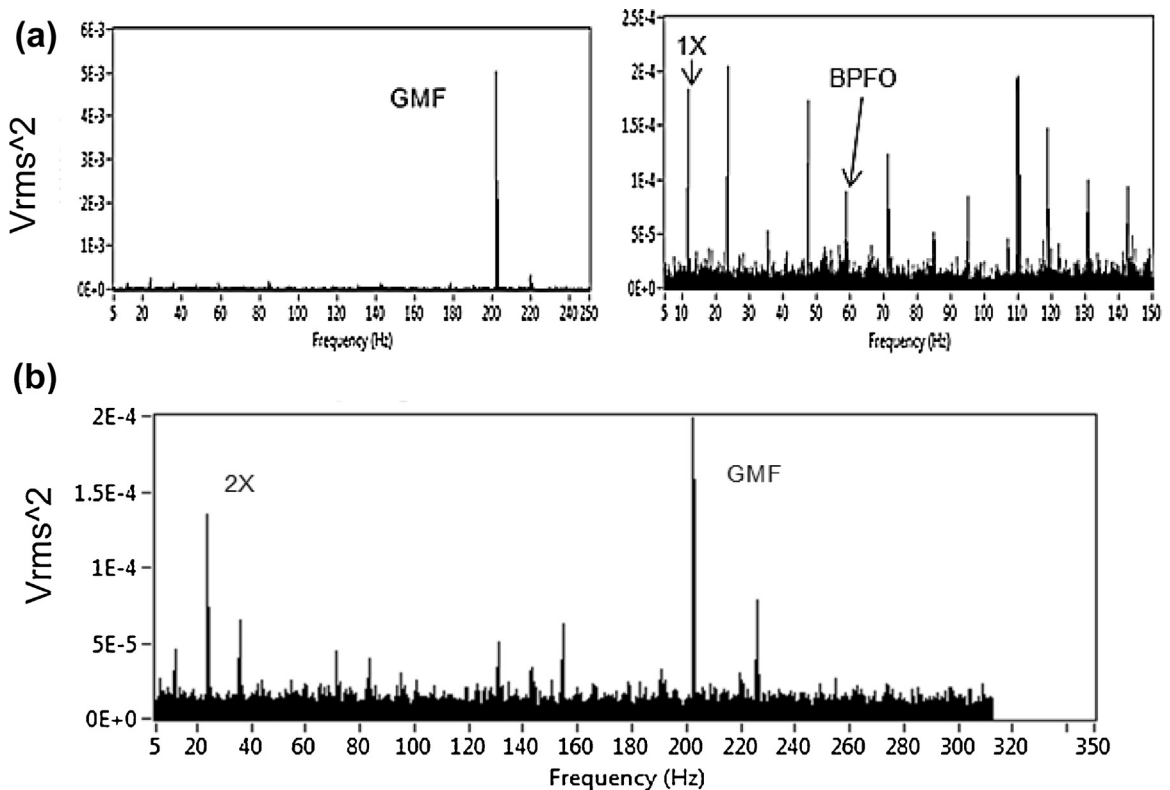


Fig. 3. (a) Enveloped signal spectrum with LMS algorithm at 24% of life and (b) Enveloped signal spectrum using a FBLMS algorithm at 24%.

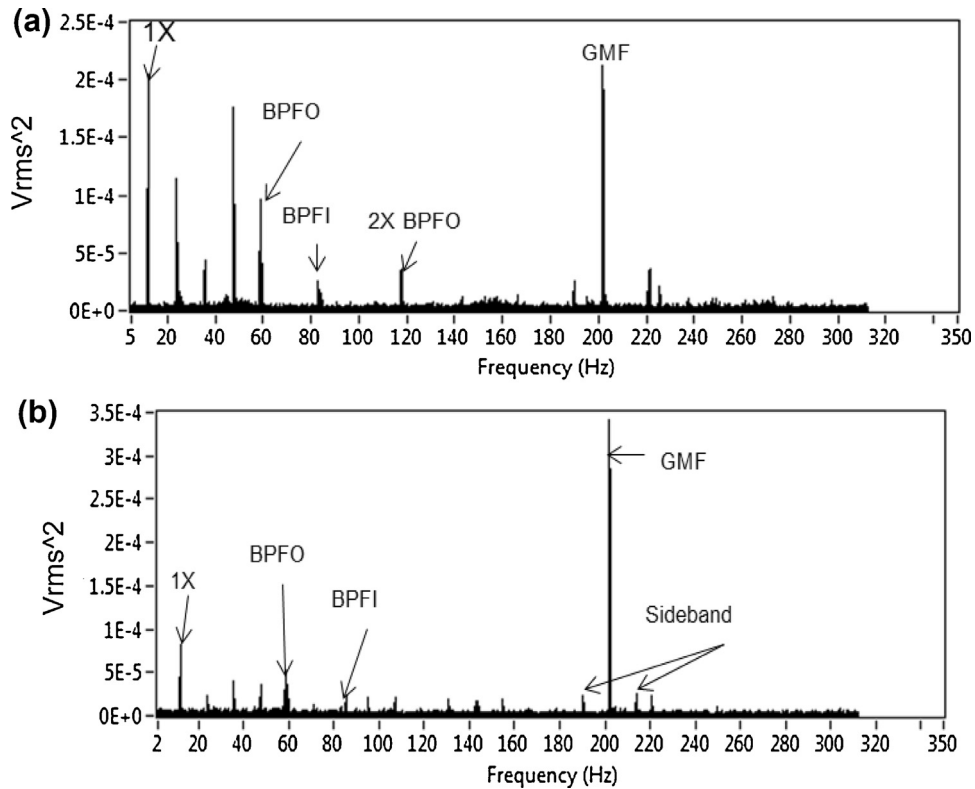


Fig. 4. (a) Enveloped signal spectrum with LMS algorithm at 27% of life and (b) Enveloped signal spectrum with FBLMS algorithm at 27% of life.

of the SK. On identification of the frequency band in which the SK is maximized, this information can be used to design a filter which extracts the part of the signal with the highest level of impulsiveness. The filtered signal can be finally used to perform an envelope analysis, which is a widely used technique for identification of modulating frequencies related to bearing faults. In this investigation the SK computation and the subsequent signal filtration and envelope analysis were performed using the original Matlab code programmed by Antoni [20].

### 3. Experimental setup

The gearbox considered is used as part of a transmission driveline on the actuation mechanism of secondary control surfaces in civil aircrafts. The test rig was designed to simulate the actual operation conditions during the life cycle of the aircraft control system which implies the gearbox would experience a range of speed and torque conditions. The test rig was driven by an electrical motor. A second motor, which acted as a generator, was employed to apply a range of loading conditions. These conditions included the simulation of takeoff and landing with different flap positions. A schematic of the testing is presented in Fig. 1 and load conditions are summarized in Table 1. The motor nominal speed was 710 rpm and the expected life of the bearing under this condition is 3000 h. The gearbox consists of two spur bevel gears as shown in Fig. 1, each gear with 17 teeth producing a gear ratio of 1:1. Two angular contact bearings are used to support each gear. During an endurance test of the flight system, a bearing within the gearbox failed after 860 h of testing which is approximately 30% of the expected bearing life. Vibration measurements were taken from the gearbox at different stages of the test. In addition, torque and angular velocity were also measured.

Vibration data was acquired using an accelerometer fixed on the outer case of the gearbox as shown in Fig. 1. The operating frequency range of the accelerometers was 10–10000 Hz. A signal conditioner (Endevco 2775A) was employed and an NI-DAQ system was used to acquire data at a sampling rate of 5 kHz. Data was acquired at different periods during the endurance test.

The endurance test ran continuously for 864 h and over this period the rig was stopped at certain periods for bearing inspection after which the rig was reassembled and the test sequence resumed. Vibration data was recorded at all test stages, however for this paper a representative data set was selected, that corresponded to 720, 810 and 864 h into the endurance test corresponding to 24%, 27% and 30% of bearing life respectively. Each vibration measurement had a duration of 210 s sampled at 5 kHz. The duration of the vibration data represented the complete load cycle. The data under maximum torque was selected for processing. The main rotational frequencies and bearing faults frequencies are summarized in Table 2.

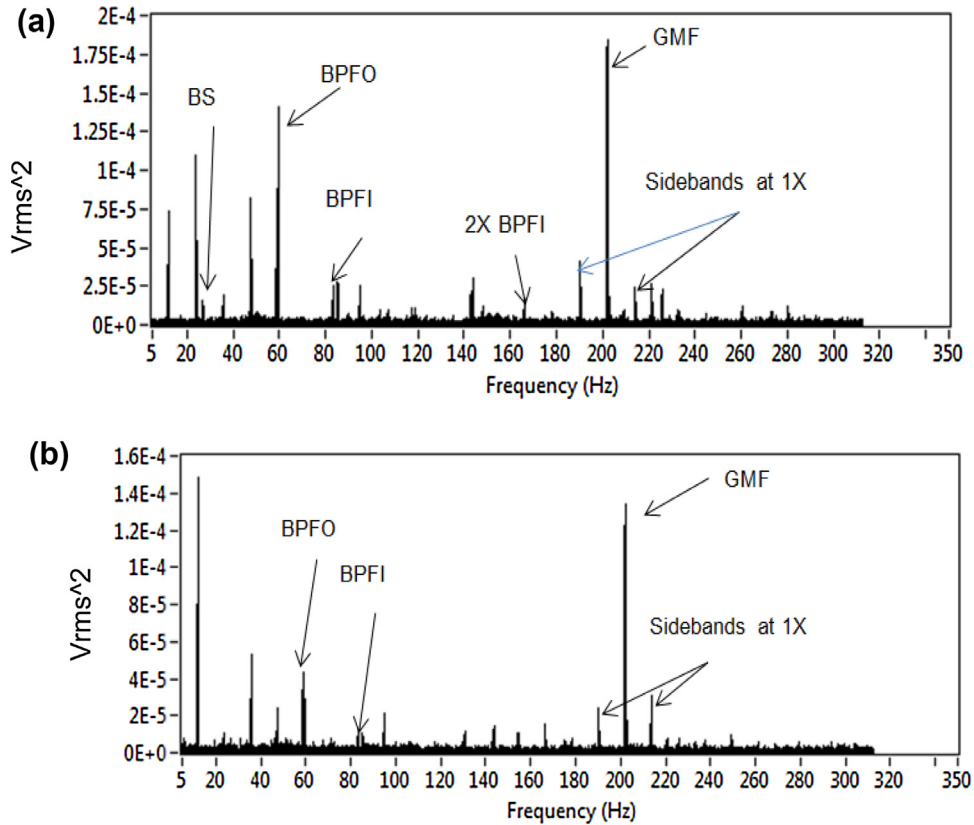


Fig. 5. (a) Enveloped signal at 30% of life using LMS algorithm and (b) Enveloped signal spectrum at 30% of life using FBLMS algorithm.

#### 4. Proposed comparison approach

For the comparative analysis the vibration signatures acquired were processed by the signal separation algorithms prior to the use of spectral kurtosis to specify the optimum filter characteristics of the non-deterministic component of the signature for envelope analysis. Lastly the frequency spectrum of the enveloped signal was determined. The performance comparison of signal separation algorithms was based on ability of each algorithm to detect the fault at earliest stage.

#### 5. Result and observations

##### 5.1. Spectral kurtosis

Analysis employing spectral kurtosis was undertaken on all data set after signal separation, this yielded the frequency band and centre frequency which were then used to undertake the envelope analysis. The defaults of the centre frequencies are shown in Table 3. These frequencies were employed for envelop analysis in this section and for enveloping the separated signal obtained from SANC, LMS and FBLMS algorithms.

##### 5.2. SANC algorithm

From analysis and observations Fig. 2(a) background noise was reduced following implementation of the SANC algorithm, increasing clearly the signal to noise ratio by approximately 43% and facilitating the identification of the different signal components. The original spectrum of the second observation (see Fig. 2(b)) shows the same components as noted in the first observation, with the difference being that there is a reduction in the amplitude of the peaks and the background noise is slightly lower. No new signal components were identified by SANC, despite the reduction in background noise reduction; an improvement of the 16.5% in the signal to noise ratio in comparison with the original signal. For the third observation (30% of bearing life) (see Fig. 2(c)) showed that even under this low torque condition, and despite the reduction in amplitude, all previously noted peaks were evident in the original spectrum, in addition to a clear peak at 58.8 Hz, indicating the defect in the outer race of the bearing.

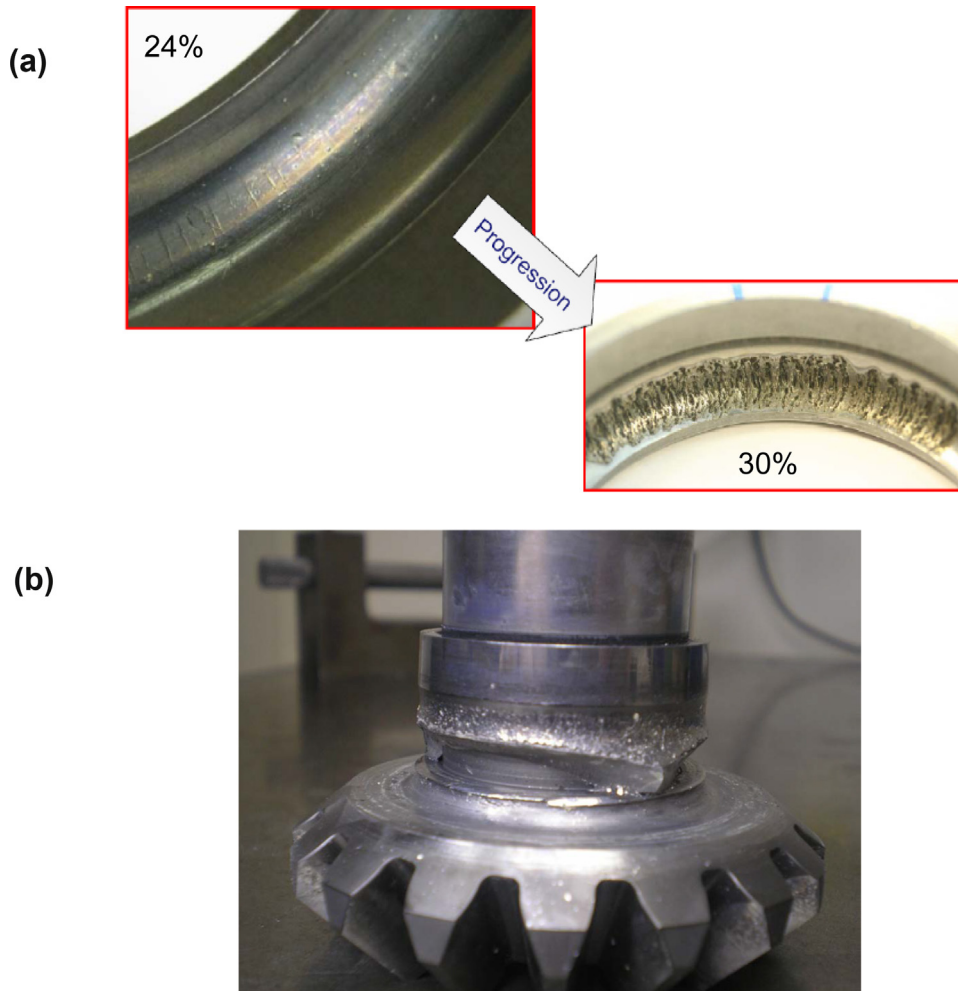


**Fig. 6.** (a) Bearing failure progress at 24% and 30% of life time and (b) Inner race damaged at the end of the test.

### 5.3. LMS and FBLMS results

After the bearing signal separation had been completed, envelop analysis was performed to identify any bearing defect frequencies. The envelop analysis was performed by applying a band-pass filter centered around 2083 Hz with a bandwidth of 833.33 Hz. These parameters were selected based on the result from maximum spectral kurtosis as described in Section 5.1.

The spectrum of enveloped signal associated with 24% of bearing life is presented in Fig. 3(a) for the LMS algorithm. Observations showed the gear mesh (201.1 Hz) was dominant (see left plot in Fig. 3). The right plot in Fig. 3(a) represents a narrower frequency range in the original spectrum showing the presence of BPFO, shaft speed and harmonics of shaft speed. Fig. 3(b) shows the result obtained by enveloping the FBLMS algorithms, which does not show the existence of any fault frequencies at this stage.

The spectrum of the enveloped signal from the second data (27% of bearing life) using the LMS algorithm is shown in Fig. 4(a). The presence of the outer race defect frequency was evident; in addition a second harmonic of the BPFO was noted (118 Hz). This result supports the observation obtained from the first data set (see Fig. 3). Furthermore, the bearing inner race defect was also identified at 83.2 Hz as shown in Fig. 4(a).

Result from processing the data at 27% using FBLMS algorithms showed the presence of both BPFI and BPFO frequencies at 58.85 and 83.2 Hz respectively see Fig. 4(b). In addition, side-bands around gear mesh spaced by shaft frequency and shaft harmonics were identified by both algorithms as shown in Fig. 4(b).

For data set collected at 30% of bearing life, the frequency spectrum obtained from the LMS algorithms showed BPFO, BPFI, and Ball Spin (BS) frequencies, see Fig. 5(a). In addition the second harmonic of the BPFI frequency (165 Hz) was evident. The frequency spectrum obtained from the FBLMS algorithms showed BPFI and BPFO frequencies as shown in Fig. 5(b). Fig. 5 shows side-bands around fundamental gear mesh spaced by shaft frequency and shaft harmonics were now more

pronounced in the spectrum for the data set associated with 30% bearing life, this is indicative of misalignment. This misalignment can affect the gear mesh and further accelerate bearing degradation, consequently the test was stopped at this stage and a visual inspection was performed to assess the damage.

At all three life stages the gearbox was disassembled for visual inspection, evidence of scratches in the bearing outer race at an early stage of 24% was observed, see Fig.6(a). At the end of the test the bearing ball and outer race were damaged as shown in Fig. 6(b).

## 6. Concluding remarks

The techniques used in this paper are typically used for applications where strong background noise masks the defect signature of interest within the measured vibration signature. Of all the techniques presented, the LMS algorithm succeeded in detecting the bearing outer race fault earliest at 24% of bearing life. FBLMS technique detected the bearing outer race fault at 27% of bearing life. In addition, the LMS algorithm was the only technique that successfully identified both the outer race and ball spin faults. The SANC algorithm detected the fault at 30% of bearing life, though SANC showed its capability in reducing the background noise and facilitating the identification of the different components in the signal spectrum.

A comparison of the LMS and FBLMS algorithms showed that LMS is able to detect the bearing fault earlier than FBLMS. However, the computational cost for LMS is high and therefore FBLMS is more suitable for online diagnostics where an immediate response is required. On the other hand, LMS can be used for offline diagnostics. The latter could be employed in instances where the rate of monitoring is sufficiently spaced, for instance, in tidal turbine applications where vibration data is acquired at several hours' intervals. Under such scenarios the LMS algorithm is best suited for diagnosing bearing faults in gearboxes. It is worth noting that these algorithms provide superior fault detection at early stages of degradation, however the fault size and severity cannot be ascertained with these techniques.

## References

- [1] R.B. Randall, J. Antoni, Rolling element bearing diagnostics—a tutorial, *Mech. Syst. Sig. Process.* 25 (2) (2011) 485–520.
- [2] C.K. Tan, P. Irving, D. Mba, A comparative experimental study on the diagnostic and prognostic capabilities of acoustics emission, vibration and spectrometric oil analysis for spur gears, *Mech. Syst. Sig. Process.* 21 (1) (2007) 208–233.
- [3] Randall R. B., Tech B. (2004), Cepstrum Analysis and Gearbox Fault Diagnosis, [Online], no. 2nd edition, pp. 10/07/2012 available at: [www.bksv.com/doc/233-80.pdf](http://www.bksv.com/doc/233-80.pdf).
- [4] A.M. Al-Ghamd, D. Mba, A comparative experimental study on the use of acoustic emission and vibration analysis for bearing defect identification and estimation of defect size, *Mech. Syst. Sig. Process.* 20 (7) (2006) 1537–1571.
- [5] P.D. McFadden, M.M. Toozhy, Application of synchronous averaging to vibration monitoring of rolling elements bearings, *Mech. Syst. Sig. Process.* 14 (6) (2000) 891–906.
- [6] I. Howard, A review of rolling element bearing vibration detection, diagnosis and prognosis, Department of Defense, 1994 DSTO-RR-0013.
- [7] N. Sawalhi, R.B. Randall, H. Endo, The enhancement of fault detection and diagnosis in rolling element bearings using minimum entropy deconvolution combined with spectral kurtosis, *Mech. Syst. Sig. Process.* 21 (6) (2007) 2616–2633.
- [8] P.D. McFadden, J.D. Smith, Vibration monitoring of rolling element bearings by the high-frequency resonance technique—a review, *Tribol. Int.* 17 (1) (1984) 3–10.
- [9] T. Barszcz, Decomposition of vibration signals into deterministic and nondeterministic components and its capabilities of fault detection and identification, *Int. J. Appl. Math. Comput. Sci.* 19 (2) (2009) 327–335.
- [10] M.S. Carney, J.A. Mann III, J. Gagliardi, Adaptive filtering of sound pressure signals for monitoring machinery in noisy environments, *Appl. Acoust.* 43 (4) (1994) 333–351.
- [11] J. Antoni, R.B. Randall, Unsupervised noise cancellation for vibration signals: part I—evaluation of adaptive algorithms, *Mech. Syst. Sig. Process.* 18 (1) (2004) 89–101.
- [12] B. Widrow, J.R. Glover Jr., J.M. McCool, J. Kaunitz, C.S. Williams, R.H. Hearn, J.R. Zeidler, J. Eugene Dong, R.C. Goodlin, Adaptive noise cancelling: principles and applications, *Proc. IEEE* 63 (12) (1975) 1692–1716.
- [13] G.K. Chaturved, D.W. Thomas, Adaptive noise cancelling and condition monitoring, *J. Sound Vib.* 76 (3) (1981) 391–405.
- [14] D. Ho, R.B. Randall, Optimisation of bearing diagnostic techniques using simulated and actual bearing fault signal, *Mech. Syst. Sig. Process.* 14 (5) (2000) 763–788.
- [15] S.C. Douglas, M. Rupp, Convergence Issues in the LMS Adaptive Filter, in: V.K. Madiseti (Ed.), *The Digital Signal Processing Handbook*, 2nd ed., CRC Press, Atlanta, USA, 1999.
- [16] F. Elasha, C. Ruiz-Carcel, D. Mba, P. Chandra, A comparative study of the effectiveness of adaptive filter algorithms, spectral kurtosis and linear prediction in detection of a naturally degraded bearing in a gearbox, *J. Fail. Anal. Prev.* 14 (5) (2014) 623–636.
- [17] B. Widrow, J. McCool, M. Ball, The complex LMS algorithm, *Proc. IEEE* 63 (4) (1975) 719–720.
- [18] M. Dentino, J. McCool, B. Widrow, Adaptive filtering in the frequency domain, *Proc. IEEE* 66 (12) (1978) 1658–1659.
- [19] E.R. Ferrara, Fast implementations of LMS adaptive filters, *Acoust. Speech Signal Process. IEEE Trans. on* 28 (4) (1980) 474–475.
- [20] J. Antoni, Fast computation of the kurtogram for the detection of transient faults, *Mech. Syst. Sig. Process.* 21 (1) (2007) 108–124.